Decolorization of Indigo Carmine Solution by Dielectric Barrier Discharge

K. Teranishi[1], K. Yoshioka[1], A. Sohda[1], K. Murata[1], N. Shimomura[1], H. Itoh[2]

[1]*Tokushima University, 2-1 Minami-Josanjima, Tokushima 7708506 Japan*
[2]*Chiba Institute of Technology, 2-17-1 Tsudanuma, Narashino 2750016 Japan*

A dielectric barrier discharge (DBD) plasma reactor for the water treatment was developed, which employed a parallel plate electrode configuration with the gap length of 1-2.5 mm. The treating water ejected onto the plane electrode surface forms a water film with the water flow rate of 1.7 L/min, which is exposed to the DBD plasma. The decolorization of the indigo carmine solution was carried out with feeding the air and Ar into the DBD plasma. The water film thickness was measured by a height gauge. The dependence of the discharge gas and the gap distance on the decolorization was also investigated.

1. Introduction

Advanced oxidation process (AOP) [1] is the prominent technology for water treatment, which is able to decompose persistent organic compounds, such as dioxins and inclusions in the drug medicine and the agricultural chemicals. In the AOPs, the hydroxyl (OH) radical synthesized by the reactions between ozone and H_2O_2 or an UV irradiation plays the main role of the degradation of the pollutants since it can completely break almost all the chemical bonding in the organic compounds due to its high oxidation potential.

Recently, studies on the water treatment aiming to decompose the persistent organic compounds by the discharge plasma produced directly on a water surface or inside gas bubbles in water have been actively done by many researchers [2]. Although this kind of treatment can be classified into the AOP in terms of utilizing the OH radicals, the direct excitation of the discharge plasma on/in water can offer more aggressive plasma-chemical reactions between water and plasma species such as energetic electrons, photons and chemically active species including the OH radicals.

Various configurations of the plasma reactors have been proposed for the water treatment, such as that using the pulsed discharge ignited within bubbles in water [3]–[5] or spraying water droplets [6] and corona discharge produced over the water surface [7], [8]. However, there exist few studies on the water treatment utilizing a dielectric barrier discharge (DBD) plasma except for the papers reported by Kuraica *et al* [9]–[12]. The DBD has been widely applied to the ozone generators for many years, which can synthesize large quantity of ozone with high concentration. Hence, for the water treatment by the DBD, the plasma involving the high-concentration ozone and the atomic oxygen can be exerted directly on the water surface, which leads to promote the improvement of water treatment. However, there would be considerable difficulty in generating the DBD stably on the water surface because of the short gap configuration necessary to excite the DBD. Despite such difficulty, the water falling film DBD reactors proposed by Kuraica *et al.* [9]–[12] are reasonably designed to expose the DBD to the water surface. They have used a coaxially cylindrical electrode configuration. The water film that spills out of the top of the inner cylinder electrode flows down on its outer electrode surface with the water flow rate of 80–580 mL/min [9], which is exposed to the DBD plasma.

In this study, a DBD plasma reactor for the water treatment was also constructed and studied, which employed a parallel plate electrode configuration. The treating water is ejected onto a flat plate electrode surface to form the water film. The present DBD reactor has the advantage of being able to treat the large flow of water up to 1.7 L/min. This paper presents some of the experimental results concerning the decolorization of the indigo carmine solution performed in order to evaluate the characteristics of the water treatment. The water film thickness was measured by a height gauge. The dependence of the kind of discharge gas and the gap distance on the decolorization was also investigated.

2. Experimental

2.1. DBD plasma reactor

Figure 1 shows the configuration of the DBD plasma reactor for the water treatment. The plasma reactor consists mainly of the upper and lower electrodes, a dielectric barrier, the water inlet and outlet, the gas inlet and outlet, the storage tank and the water pump. The upper electrode is a doughnut-shaped copper foil with an inner diameter of 26 mm and an outer diameter of 50 mm. The copper foil electrode is attached on the circular dielectric barrier with a 75-mm diameter and a 1-mm thickness. The lower electrode is a stainless-steel circular plate with a diameter of 52 mm, which connects to ground through a 10-nF capacitor. Sinusoidal high-voltage of 5.0–7.2 kV with a frequency of 18 kHz is applied using a neon-invertor transformer. The discharge gas is fed from the gas inlet into the discharge space. The indigo carmine solution is provided from the water inlet and then ejected from the feed-water nozzle through an 8-mm hole of dielectric barrier, which results in the water film on the lower electrode surface. The DBD appears between the dielectric barrier surface and the water film. The gap distance d_g between the dielectric barrier and lower electrode surfaces is variable by rotating the screw bolt attached under the lower electrodes. In this study, the experiment was carried out for the different gap distance of 1–2.5 mm. The treated solution is impounded in a storage tank and then circulated by the water pump with the flow rate of 1.7 L/min. In this study, we prepared a 400-mL indigo carmine solution with 20 mg/L in the concentration. The decolorization rate of the treated indigo carmine solution was evaluated by the absorbance spectra measured by the VIS/UV spectrophotometer. The discharge power of the DBD was estimated by the Q–V Lissajous figure method.

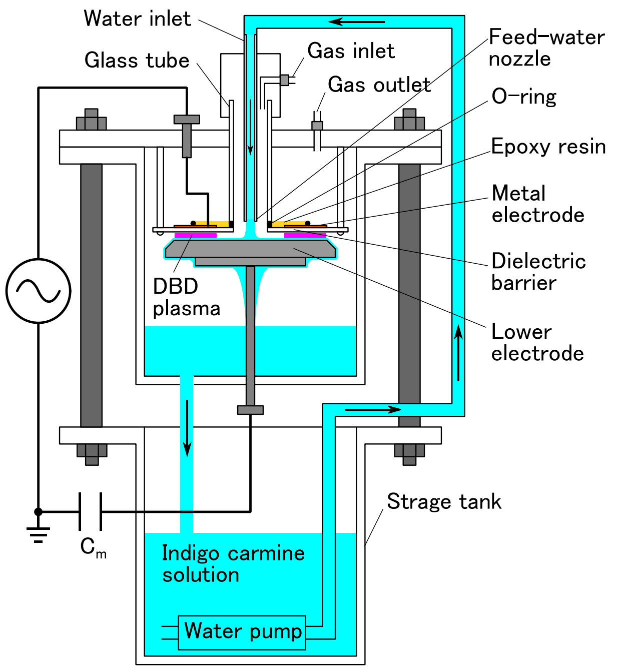

Fig. 1 Configuration of the water treatment DBD reactor

2.2. Formation of water film

In the present plasma reactor shown in Fig. 1, if the water pump is repeatedly driven to flow the water in the short gap space, the upper dielectric barrier surface gets wet with the water rebound from the opposite lower electrode even though the water film can be stably formed. In the longer gap distance more than 2 mm, the water film can be formed and the stable DBD appears by the operation after several tens of seconds until the dielectric barrier dries. However, in the gap distance less than 1.5 mm, just driving the water pump fails to form the water film since the water comes into contact with the upper dielectric barrier surface. This leads to the failure of the discharge ignition. Therefore, in this study, before the water pump was activated, we once adjusted the gap distance to be long enough to avoid the water contact with the dielectric barrier surface. After that, the water pump was activated to form the water film and then the gap distance was shortened until it reaches desired gap length.

3. Experimental results and discussions

3.1. Thickness of water film

We first estimated the thickness of the water film formed on the lower electrode surface. Figure 2 shows the measurement system for the water film thickness. The acrylic rod ($3\times3\times300$ mm^3) is mounted on the scriber of the height gauge and inserted into the reactor, which is perpendicular to the lower electrode surface. Therefore, the bottom surface of the rod serves as the reference level of the height measurement. Without the water film, the height of the acrylic rod is adjusted carefully to make its bottom surface contact with the lower electrode surface and the indicated value of the gauge is defined as the height of the lower electrode surface h_0. Similarly, with forming the water film, the indicated value, in which the rod bottom surface makes contact with the water film surface, is as the height of the water film and the lower electrode surface h_1. Consequently, the thickness of the water film h_w can be evaluated by $h_w = h_1 - h_0$. This measurement was repeated five times and the results are obtained to be 0.50, 0.50, 0.38, 0.38 and 0.46 mm. Consequently, the average value of the water film thickness is estimated to be 0.44 mm.

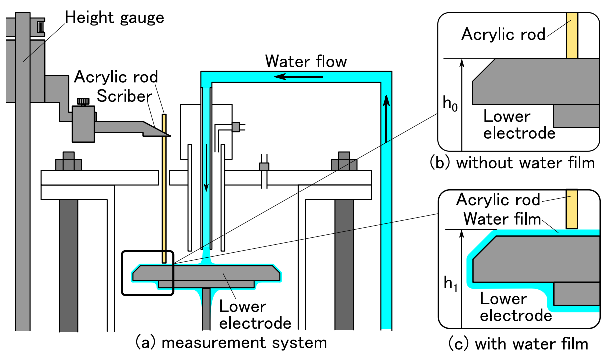

Fig. 2 Measurement of water film thickness

3.2. Temporal variations of absorbance spectra

Figures 3(a) and (b) show the temporal variation of the absorbance spectra of the indigo carmine solution, which were obtained by feeding Air and Ar as the discharge gas, respectively. In this experiment, a glass-composite plate, which has been widely used as electrical circuit board, was employed as the dielectric barrier. The gap distance was adjusted to be 1.5 mm. The discharge power was 15.6 and 6.65 W for the discharge gas of the air and Ar, respectively. The absorbance spectrum before the plasma treatment (0 min) is represented by the black curve and that with the plasma treatment is by the colored curves. Before the plasma treatment, the absorbance spectrum has four peaks at 207, 252, 287 and 609 nm. Among these absorbance peaks, the peak at 609 nm indicates the decolorization degree of blue color in the indigo carmine solution. When the air is used as the discharge gas, the absorbance peaks at 609 and 287 nm decrease with the treatment time. In particular, the peak at 609 nm becomes almost zero by a 6-minutes plasma treatment. In contrast, the peaks at 207 and 252 nm increase with the treatment time. The increase of these absorbance peaks is thought to be due to some sort of products during the plasma treatment. In the case of the Ar discharge gas, the absorbance peaks at 252, 287 and 609 nm decrease and that at 207 nm slightly increases with the treatment time. The absorbance at 609 nm reaches almost zero by a 60-minutes discharge treatment, which is quite longer than by the air plasma treatment. Also, the absorbance spectra obtained after the plasma treatment by the air and Ar discharge gases show the different trends. These results indicate that the decomposition process of the indigo carmine solution depends upon the kind of discharge gas fed into the reactor.

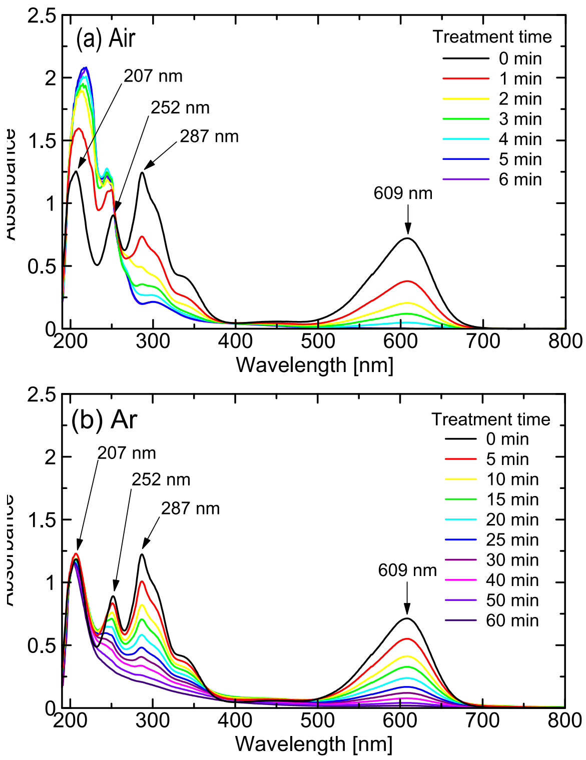

Fig. 3 Temporal variation of the absorbance spectra obtained by the air and Ar discharge gas

3.3. Decolorization rate at 609 nm

Figure 4 shows the decolorization rate of the indigo carmine solution at 609 nm plotted with respect to the consumption energy into the plasma reactor. The decolorization rate at 609 nm D_{609} is evaluated by the following equation,

$$D_{609} = \frac{A_0 - A_t}{A_0} \times 100\ [\%], \qquad (1)$$

where A_0 and A_t are the absorbance before the plasma treatment and after that for a certain period of time t. The consumption energy E is calculated by the product of discharge power P and the plasma treatment time t. The decolorization rate increases with increasing the consumption energy for both discharge gases. The decolorization rates by feeding the air and Ar are obtained to be 99.9 and 97.3% with the energy consumptions at 1.56 and 6.65 Wh, respectively. Hence, by feeding the air as the discharge gas, the decolorization of the indigo carmine at 609 nm can be done with the lower energy consumption than that by feeding Ar.

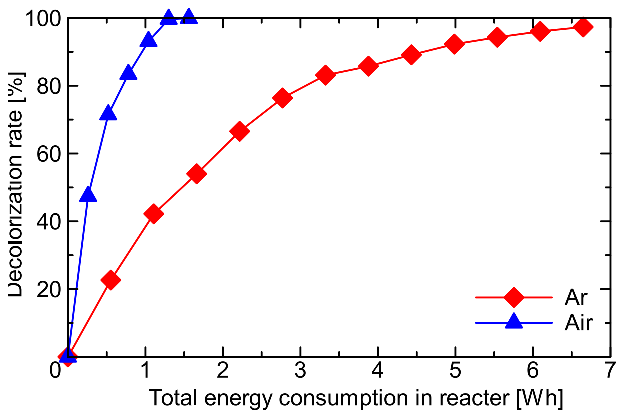

Fig. 4 Decolorization vs. total energy consumption obtained by the air and Ar discharge gas

3.4. Dependence of gap distance on decolorization

The dependence of the gap distance on the decolorization rate was investigated. In this experiment, a Pyrex glass plate was used as a dielectric barrier and the discharge gas was the air. For all gap distances, the experiments were performed by fixing the primary current of the neon invertor transformer. Electrical characteristics estimated from the Lissajous figures are listed in Table 1. When increasing the gap distance, the applied voltage and the discharge power also become large. Figure 5(a) shows the temporal variation of the decolorization rate obtained for the different gap distance. The increase in the decolorization late with the treatment time does

Table 1 Electrical characteristics estimated from Lissajous figure

Gap distance d_g (mm)	1	1.5	2	2.5
Applied voltage (kV)	4.95	4.89	6.11	7.23
Frequency (kHz)	18.3	18.5	18.2	18.4
Discharge power (W)	6.78	8.02	22.2	34.6

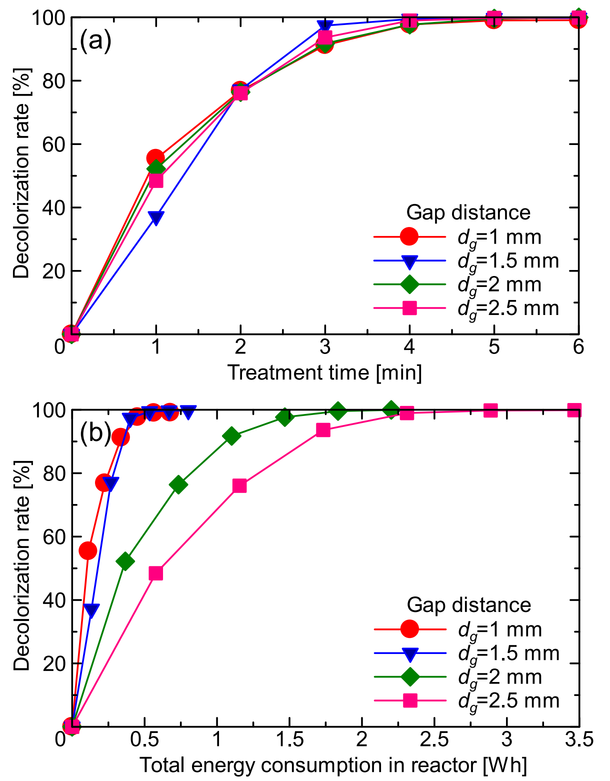

Fig. 5 Dependence of gap distance on decolorization rate of indigo carmine solution

not depend on the gap distance even though the discharge power increases with increasing the gap distance. Therefore, the higher decolorization rate with lower consumption energy is obtained with the short gap distance as shown in Fig. 5(b), which leads to improve the decolorization efficiency. We have not yet understood the reason why the short gap distance exhibits the high decolorization efficiency of the indigo carmine. However, the plasma species, such as reactive oxygen species and energetic electrons and photons, effective for the water treatment can be expected to exist in the DBD plasma with short gap condition. Further detailed investigations are absolutely necessary.

4. Conclusions

The decolorization of the indigo carmine was investigated to evaluate the characteristics of the water treatment by the DBD plasma reactor employed a parallel plate electrode configuration. The thickness of the water film formed on the lower electrode surface can be estimated to be 0.44 mm with the water flow rate of 1.7 L/min. The absorbance spectra obtained after the plasma treatment by the air and Ar discharge gases show the different trends. Therefore, the decomposition process of the indigo carmine solution depends on the kind of the discharge gas. For the decolorization of the indigo carmine at 609 nm, the air-fed DBD plasma is more efficient than the Ar-fed DBD plasma. The higher decolorization rate with lower consumption energy is obtained with the short gap distance.

5. References

[1] Carla C. A. Loures *et al.*, *International Review of Chemical Engineering* **5** (2013) 102−120 .

[2] B. R. Locke *et al.*, *Ind. Eng. Chem. Res.* **45** (2006) 882−905.

[3] C. Yamabe *et al.*, *Plasma Process. Polym*. **2** (2005) 246−251.

[4] K. Yasuoka and Y. Satoh, *Int. J. Plasma Env. Sci. and Technol.* **3** (2009) 22−27.

[5] F. Fukawa *et al.*, *IEEE Trans. Plasma Sci.* **39** (2011) 2662−2663.

[6] T. Kobayashi *et al.*, *IEEE Trans. Plasma Sci*. **38** (2010) 2675−2680.

[7] W. F. L. M. Hoeben *et al.*, *Plasma Sources Sci. Technol*. **9** (2000) 361–369.

[8] H. Shiota *et al.*, *IEEJ Trans. FM* **132** (2012) 297−304 *in Japanese*.

[9] M. M. Kuraica *et al.*, *Vacuum*, **73** (2004) 705–708.

[10] B. P. Dojčinović *et al.*, *Vacuum* **83** (2009) 234−237.

[11] B. P. Dojčinović *et al.*, *J. Hazardous Materials* **192** (2011) 763−771.

[12] M. S. Jović *et al.*, *Chem. Eng. J.* **248** (2014) 63–70.